Polarization interference mapping of microscopic images of protein fluorofores in the differential diagnosis of benign and malignant prostate tumours

Trifonyuk[1] L., Strashkevich[2] A., Pavlyukovich[3] N., Pavlyukovich[3] A.,
Tomka[4] Yu., Zhitaryuk[4] V., Tkachuk[4] V. I.

[1] Rivne State Medical Hospital, Rivne, Ukraine
[2]The Institute of Traumatology and Orthopedics by NAMS of Ukraine, Kyiv, Ukraine
[3]Bukovinian State Medical University, Chernivtsi, Ukraine
[4]Chernivtsi National University, Chernivtsi, Ukraine

ABSTRACT

The paper presents the results of the possibility of a polarization-interference approach to the analysis of microscopic images of biological preparations in the differential diagnosis [1-7] of benign and malignant prostate tumors with different degrees of differentiation. Measurements and analysis of maps and histograms of the distribution of the local contrast value of polarization-interference distributions of microscopic images of biological preparations of the prostate. Determination of the relationship between the statistical moments of the 1st - 4th orders, characterizing the distributions of the value of the local contrast of polarization-interference distributions of microscopic images of biological preparations of the prostate [8-12]. Determination of statistical criteria for polarization-interference diagnosis of histological sections of biopsy of adenoma and adenocarcinoma of the prostate with varying degrees of differentiation. Determination of operational characteristics (sensitivity, specificity, accuracy) of the diagnostic power [13-19] of the polarization interferometry method for differential diagnosis of histological sections of biopsy of adenoma and adenocarcinoma of the prostate with varying degrees of differentiation.

Keywords: laser, polarization, interference, image, fluorophore, statistical moments of the 1st-4th orders, adenoma, adenocarcinoma, sensitivity, specificity, accuracy

1. CHARACTERISTICS OF RESEARCH OBJECTS

The following groups of prostate tissue samples were studied:

1. Histological sections of prostate adenoma biopsy control group 1 (36 samples).
2. Histological biopsy sections of highly differentiated adenocarcinoma (3 + 3) of the prostate - study group 2 (36 samples).
3. Histological biopsy sections of medium differentiated adenocarcinoma (3 + 4) of the prostate - study group 3 (36 samples).
4. Histological biopsy sections of low differentiated adenocarcinoma (4 + 4) of the prostate - study group 4 (36 samples).

2. THE TECHNIQUE OF POLARIZATION-INTERFERENCE MAPPING OF THE FIELD OF COMPLEX AMPLITUDES IN THE PLANE OF THE MICROSCOPIC IMAGE OF PROSTATE TUMOUR PREPARATIONS

The technique of polarization-interference mapping of the field of complex amplitudes in the plane of the microscopic image of the biological layer consists in the following set of actions:

Fifteenth International Conference on Correlation Optics, edited by Oleg V. Angelsky, Proc. of SPIE Vol. 12126, 1212628
© 2021 SPIE · 0277-786X · doi: 10.1117/12.2616836

- Simultaneous formation of right-circularly polarized states in the "irradiating" and "reference" parallel laser beams.
- Registration of the coordinate distribution of intensity of the interference pattern in the plane of a set of pixels ($\mathrm{m}\times\mathrm{n}$) of a digital camera 14.
- By scanning along the lines ($\begin{Bmatrix}1,2,3,.....n;\\.....;\\m,\mathrm{m}+1,...n\end{Bmatrix}$) of points with a step $1\mathrm{pix}$, the intensity values of neighboring points of the interference distribution are measured $\mathrm{I}(\mathrm{r})$ and $\mathrm{I}(\mathrm{r}+1\mathrm{pix})$.
- For each pair of points, the value of the local contrast is calculated by the ratio

$$W(r,r+1pix)=\frac{|I(r)-I(r+1pix)|}{I(r)+I(r+1pix)} \tag{1}$$

and a map of the local contrast $W(m\times n)$ of the interference distribution of the polarization-inhomogeneous microscopic image of the biological layer is obtained.

3. COORDINATE AND STATISTICAL STRUCTURE OF LOCAL CONTRAST MAPS OF MICROSCOPIC IMAGES OF HISTOLOGICAL SECTIONS OF BIOPSY OF PROSTATE TUMOURS WITH DIFFERENT DEGREES OF DIFFERENTIATION

Coordinate (fragments (1)) and statistical parameters of histograms (fragments (2)) of the distributions of the magnitude $\mathrm{W}(\mathrm{m},\mathrm{n})$ of digital microscopic images of histological sections of biopsy of adenoma and adenocarcinoma with different degrees of differentiation are shown in a series of fragments in Fig. 3 - Fig. 6

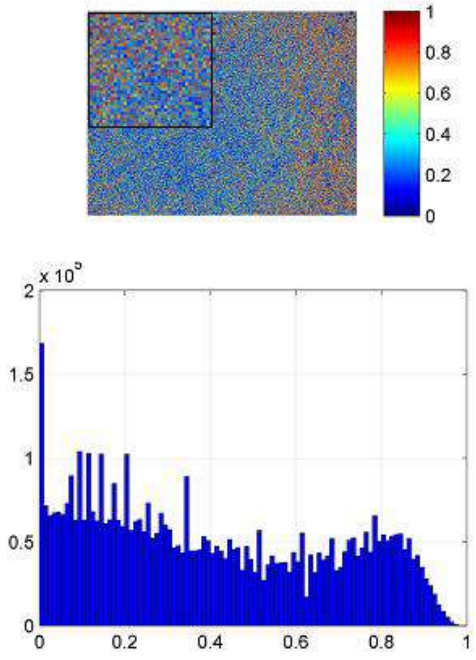

Fig. 1. Map (fragment (1)) and distribution histogram (fragment (2)) of the local contrast value of a polarization-interference microscopic image of a histological section of adenoma biopsy - control group 1.

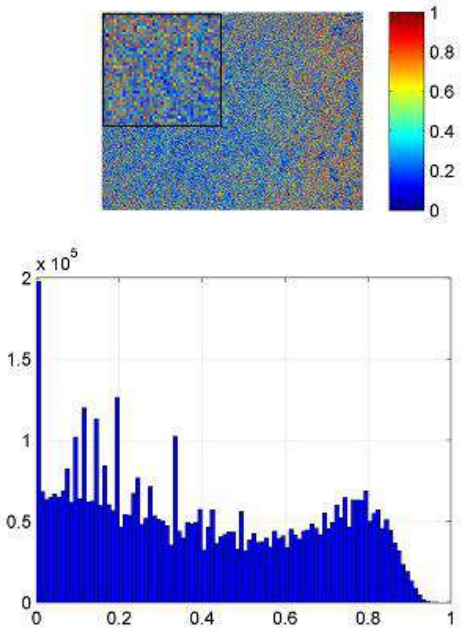

Fig. 2. Map (fragment (1)) and distribution histogram (fragment (2)) of the local contrast value of a polarization-interference microscopic image of a histological section of a biopsy of a highly differentiated adenocarcinoma (3 + 3) - study group 2.

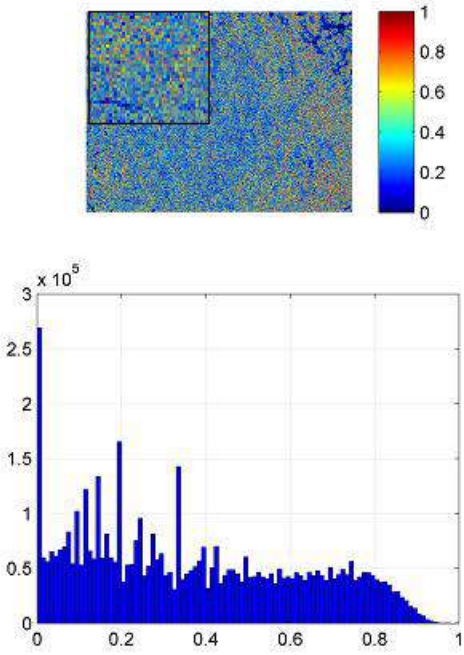

Fig. 3. Map (fragment (1)) and distribution histogram (fragment (2)) of the local contrast value of the polarization-interference microscopic image of the histological section of the biopsy of adenocarcinoma of medium differentiation (3 + 4) - study group 3.

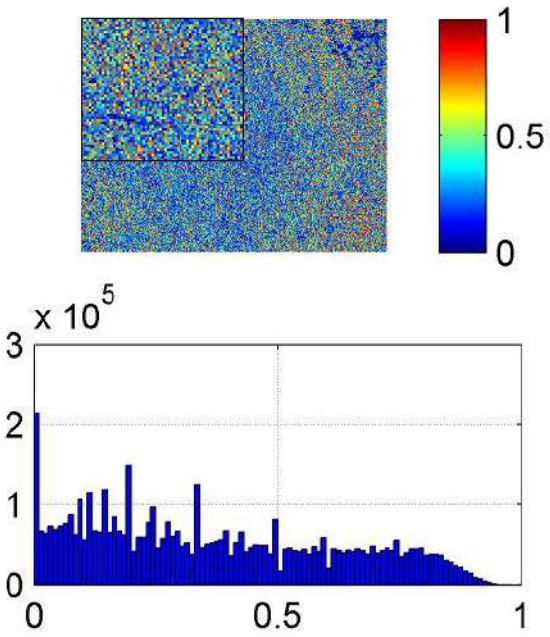

Fig. 4. Map (fragment (1)) and distribution histogram (fragment (2)) of the local contrast value of the polarization-interference microscopic image of the histological section of the biopsy of adenocarcinoma of low differentiation (4 + 4) - control group 4.

Comparative analysis of the results of polarization-interference measurement of local contrast maps (Fig. 2 - Fig. 5) of microscopic images of biological preparations of representative samples of all types of prostate tissue tumors revealed:

- The presence of the widest possible range of coordinate and quantitative changes in the magnitude of the local contrast of polarization-interference distributions in the plane of digital microscopic images of a set of histological sections of biopsy of adenoma and adenocarcinoma of the prostate of different differentiation according to the Gleason scale – (3+3), (3+4) and (4+4), - $0 \le W \le 1$.
- Individual structure of histograms of distributions of the local contrast of polarization-interference maps in the plane of digital microscopic images of a set of histological sections of a biopsy of adenoma and adenocarcinoma of the prostate of different differentiation according to the Gleason scale – (3+3), (3+4) i (4+4).
- Sequential decrease in the average histograms of distributions of the local contrast value of polarization-interference maps in the plane of digital microscopic images of histological sections of biopsy of adenoma and adenocarcinoma as the degree of differentiation on the Gleason scale decreases – (3+3), (3+4) and (4+4).

Biophysical, this can be associated with necrotic changes in the morphological structure of malignant prostate tumors, which lead to a decrease in the level of optical anisotropy of histological sections of adenocarcinoma with a decrease in the level of their differentiation. – (3+3), (3+4) and (4+4).

This scenario corresponds to a decrease in phase fluctuations at the points of digital microscopic images of histological sections of malignant tumors with low differentiation.

Therefore, one should expect the formation of an individual topographic and statistical structure with small relative values of the local contrast $W(m,n)$ of polarization-interference distributions at the points of microscopic images of histological sections of biopsy of adenocarcinoma of low differentiation

4. STATISTICAL ANALYSIS OF LOCAL CONTRAST MAPS OF DIGITAL MICROSCOPIC IMAGES OF HISTOLOGICAL SECTIONS OF BIOPSY OF PROSTATE TUMOURS WITH DIFFERENT DEGREES OF DIFFERENTIATION

Quantitatively, morphological scenarios of such necrotic processes of oncological destruction are illustrated by a set of mean intragroup values and standard deviations of the magnitude of statistical moments SM_i characterizing the distribution of the local contrast value $W(m,n)$ of digital microscopic images of representative samples of histological sections of biopsy of adenoma (control group 1) and adenocarcinoma (experimental group 2 - group 4) of various differentiation – (3+3), (3+4) and (4+4), - table1.

Table 1 Statistical parameters of the local contrast map $W(m,n)$ of microscopic images of histological sections of biopsy of benign and malignant prostate tumors

Type	Adenoma	Adenocarcinoma (3+3)	Adenocarcinoma (3+4)	Adenocarcinoma (4+4)
SM_1	0.59 ± 0.024	0.46 ± 0.021	0.35 ± 0.016	0.29 ± 0.014
p	$p \le 0.001$			
		$p \le 0.05$		
			$p \le 0.05$	
SM_2	0.37 ± 0.017	0.25 ± 0.012	0.18 ± 0.008	0.13 ± 0.006
p	$p \le 0.001$			
		$p \le 0.05$		
			$p \le 0.05$	
SM_3	0.62 ± 0.029	0.73 ± 0.034	0.88 ± 0.041	0.94 ± 0.045
p	$p \le 0.001$			
		$p \le 0.05$		
			$p \le 0.05$	
SM_4	0.49 ± 0.022	0.63 ± 0.027	0.74 ± 0.033	0.85 ± 0.039
p	$p \le 0.001$			
		$p \le 0.05$		
			$p \le 0.05$	

The statistical significance of intergroup differentiation of samples of histological sections of adenoma and carcinoma with different degrees of differentiation was carried out by cross-comparison of the magnitude of the statistical moments of the 1st - 4th orders $SM_{i=1;2;3;4}$, which characterize the distributions of the value of the local contrast of digital microscopic images of representative samples of histological sections of adenoma biopsy (control group 1) and adenocarcinoma (experimental group 2 - group 4) of various differentiation – (3+3), (3+4) and (4+4).

If the means within one of the representative set of samples of biological preparations of prostate $\overline{SM}_{i=1;2;3;4}$ are outside the standard deviation $\pm 2\Omega_{i=1;2;3;4}$ of similar values found in another group of histological sections of prostate tumor biopsies, then the difference is considered statistically significant - $p \le 0.05$ either $p \le 0.001$.

From the obtained data of the statistical analysis of local contrast distributions $W(m,n)$, which were determined by the method of polarization-interference mapping of a set of digital microscopic images, the statistical reliability of

differentiation of all types of histological biopsy sections of benign and malignant of prostate tumors with varying degrees of differentiation according to the Gleason scale (3 + 3, 3 + 4, 4 +4) was established.

5. INFORMATIONAL ANALYSIS OF THE DIAGNOSTIC POWER OF THE METHOD OF POLARIZATION-INTERFERENCE MAPPING OF MICROSCOPIC IMAGES OF HISTOLOGICAL SECTIONS OF BIOPSY OF PROSTATE TUMOURS WITH DIFFERENT DEGREES OF DIFFERENTIATION

The following results were obtained:

- Excellent level of accuracy of differential diagnosis "adenoma (control group 1) - adenocarcinoma (study group 2 - group.4)" – $Ac = 95\% \div 96\%$;
- Very good level of accuracy in the differential diagnosis of "adenocarcinoma (3 + 3, - group 2) - adenocarcinoma (4 + 4, - group 4)" – $Ac = 93\% \div 91\%$;
- Very good level of accuracy in the differential diagnosis of "adenocarcinoma (3 + 3, - group 2) - adenocarcinoma (3 + 4, - group 3)" – $Ac = 91\%$;
- A good level of accuracy in the differential diagnosis of "adenocarcinoma (3 + 4, - group 3) - adenocarcinoma (4 + 4, - group 4)" – $Ac = 85\%$.

CONCLUSIONS

1. The possibilities of the polarization-interference approach to the analysis of microscopic images of the prostate proteins fluorofores in the differential diagnosis of benign and malignant tumours experimentally investigated and clinically analyzed..
2. A complex cycle of measuring and analyzing the topographic structure of maps and histograms of the distribution of the value of the local contrast of polarization-interference distributions of digital microscopic images of a set of representative samples of biological preparations of prostate tumours of various differentiation was implemented.
3. Statistical criteria for polarization-interference diagnostics of a set of representative samples of histological sections of biopsy of adenoma and adenocarcinoma of the prostate with varying degrees of differentiation have been established and analytically substantiated.
4. As part of the information analysis, the operational characteristics (sensitivity, specificity, accuracy) of the diagnostic power of the polarization interferometry method were determined for the differential diagnosis of histological sections of the biopsy of adenoma and adenocarcinoma with varying degrees of differentiation.

FUNDING

Current research supported by the National Research Foundation of Ukraine (Project 2020.02/0061)

REFERENCES

[1] N. Ghosh and I. A. Vitkin, “Tissue polarimetry: concepts, challenges, applications and outlook,” J. Biomed. Opt. 16, 110801 (2011).
[2] S. L. Jacques, “Polarized light imaging of biological tissues” in Handbook of Biomedical Optics, D. Boas, C. Pitris, and N. Ramanujam, Eds., pp. 649–669, CRC Press, Boca Raton, London, New York (2011).
[3] N. Ghosh, M. F. G. Wood, and I. A. Vitkin, “Polarized light assessment of complex turbid media such as biological tissues via Mueller matrix decomposition,” in Handbook of Photonics for Biomedical Science, V. V. Tuchin, Ed., pp. 253–282, CRC Press, Taylor & Francis Group, London (2010).
[4] D. Layden, N. Ghosh, and A. Vitkin, “Quantitative polarimetry for tissue characterization and diagnosis,” in Advanced Biophotonics: Tissue Optical Sectioning, R. K. Wang and V. V. Tuchin, Eds., pp. 73–108, CRC Press, Taylor & Francis Group, Boca Raton, London, New York (2013).

[5] A. Vitkin, N. Ghosh, and A. de Martino, “Tissue polarimetry” in Photonics: Scientific Foundations, Technology and Applications, D. L. Andrews, Ed., Vol. IV, pp. 239–321, John Wiley & Sons, Inc., Hoboken, New Jersey (2015).
[6] S. G. Demos, H. B. Radousky, and R. R. Alfano, “Deep subsurface imaging in tissues using spectral and polarization filtering,” Opt. Express 7, 23–28 (2000).
[7] R. S. Gurjar et al., “Imaging human epithelial properties with polarized light scattering spectroscopy,” Nature Med. 7, 1245–1248 (2001).
[8] Yu. A. Ushenko, V. P. Prysyazhnyuk, M. S. Gavrylyak, M. P. Gorsky, V. T. Bachinskiy, O. Ya. Vanchuliak, "Method of azimuthally stable Mueller-matrix diagnostics of blood plasma polycrystalline films in cancer diagnostics ," Proc. SPIE 9258, Advanced Topics in Optoelectronics, Microelectronics, and Nanotechnologies VII, 925807 (20 February 2015)
[9] Ushenko, V.O., Trifonyuk, L., Ushenko, Y.A., Dubolazov, O.V., Gorsky, M.P., Ushenko, A.G. Polarization singularity analysis of Mueller-matrix invariants of optical anisotropy of biological tissues samples in cancer diagnostics (2021) Journal of Optics (United Kingdom), 23 (6), статья № 064004.
[10] Angelsky, O.V., Ushenko, Y.A., Dubolazov, A.V., Telenha, O.Yu. The interconnection between the coordinate distribution of mueller-matrixes images characteristic values of biological liquid crystals net and the pathological changes of human tissues (2010) Advances in Optical Technologies, 130659
[11] Meglinski, I., Trifonyuk, L., Bachinsky, V., Vanchulyak, O., Bodnar, B., Sidor, M., Dubolazov, O., Ushenko, A., Ushenko, Y., Soltys, I.V., Bykov, A., Hogan, B., Novikova, T. Scale-Selective and Spatial-Frequency Correlometry of Polarization-Inhomogeneous Field (2021) SpringerBriefs in Applied Sciences and Technology, pp. 33-59.
[12] Angelsky, O.V., Bekshaev, A.Y., Dragan, G.S., Maksimyak, P.P., Zenkova, C.Y., Zheng, J. Structured Light Control and Diagnostics Using Optical Crystals (2021) Frontiers in Physics, 9,715045.
[13] Angelsky, O.V., Maksimyak, P.P. Optical diagnostics of slightly rough surfaces (1992) Applied Optics, 31 (1), pp. 140-143
[14] Angelsky, O.V., Zenkova, C.Y., Hanson, S.G., Zheng, J. Extraordinary Manifestation of Evanescent Wave in Biomedical Application (2020) Frontiers in Physics, 8, 159.
[15] Angelsky, O.V., Bekshaev, A.Y., Hanson, S.G., Zenkova, C.Y., Mokhun, I.I., Jun, Z. Structured Light: Ideas and Concepts (2020) Frontiers in Physics, 8, 114
[16] Meglinski, I., Trifonyuk, L., Bachinsky, V., Vanchulyak, O., Bodnar, B., Sidor, M., Dubolazov, O., Ushenko, A., Ushenko, Y., Soltys, I.V., Bykov, A., Hogan, B., Novikova, T. Multifunctional Stokes Correlometry of Biological Layers (2021) SpringerBriefs in Applied Sciences and Technology, pp. 75-96.
[17] Meglinski, I., Trifonyuk, L., Bachinsky, V., Vanchulyak, O., Bodnar, B., Sidor, M., Dubolazov, O., Ushenko, A., Ushenko, Y., Soltys, I.V., Bykov, A., Hogan, B., Novikova, T. Methods and Means of Polarization Correlation of Fields of Laser Radiation Scattered by Biological Tissues (2021) SpringerBriefs in Applied Sciences and Technology, pp. 1-15.
[18] Meglinski, I., Trifonyuk, L., Bachinsky, V., Vanchulyak, O., Bodnar, B., Sidor, M., Dubolazov, O., Ushenko, A., Ushenko, Y., Soltys, I.V., Bykov, A., Hogan, B., Novikova, T. Materials and Methods (2021) SpringerBriefs in Applied Sciences and Technology, pp. 17-31.
[19] Trifonyuk, L., Sdobnov, A., Baranowski, W., Ushenko, V., Olar, O., Dubolazov, A., Pidkamin, L., Sidor, M., Vanchuliak, O., Motrich, A., Gorsky, M., Meglinski, I Differential Mueller matrix imaging of partially depolarizing optically anisotropic biological tissues (2020) Lasers in Medical Science, 35 (4), pp. 877-891.
[20] Ushenko, A.G., Burkovets, D.N., Ushenko, Yu.A. Polarization-Phase Mapping and Reconstruction of Biological Tissue Architectonics during Diagnosis of Pathological Lesions (2002) Optics and Spectroscopy (English translation of Optika i Spektroskopiya), 93 (3), pp. 449-456.
[21] Borovkova, M., Trifonyuk, L., Ushenko, V., Dubolazov, O., Vanchulyak, O., Bodnar, G., Ushenko, Y., Olar, O., Ushenko, O., Sakhnovskiy, M., Bykov, A., Meglinski, I. Mueller-matrix-based polarization imaging and quantitative assessment of optically anisotropic polycrystalline networks (2019) PLoS ONE, 14 (5), e0214494 .